A COMBINED LARGE-EDDY SIMULATION AND TIME-DEPENDENT RANS CAPABILITY FOR HIGH-SPEED COMPRESSIBLE FLOWS

Charles G. Speziale

September 1997

Technical Report No. AM-97-022

BOSTON UNIVERSITY

Department of Aerospace and Mechanical Engineering

110 Cummington Street
Boston, Massachusetts 02215

A COMBINED LARGE-EDDY SIMULATION AND TIME-DEPENDENT RANS CAPABILITY FOR HIGH-SPEED COMPRESSIBLE FLOWS

Charles G. Speziale

September 1997

Technical Report No. AM-97-022

REPORT DOCUMENTATION PAGE

Form Approved
OMB NO. 0704-0188

1. AGENCY USE ONLY *(Leave blank)*	2. REPORT DATE	3. REPORT TYPE AND DATES COVERED
	9/9/97	Technical Report 5/1/97 - 9/9/97

4. TITLE AND SUBTITLE

A COMBINED LARGE-EDDY SIMULATION AND TIME-DEPENDENT RANS CAPABILITY FOR HIGH-SPEED COMPRESSIBLE FLOWS

5. FUNDING NUMBERS

DAAG55-97-1-0123

6. AUTHOR(S)

Charles G. Speziale

7. PERFORMING ORGANIZATION NAMES(S) AND ADDRESS(ES)

Department of Aerospace and Mechanical Engineering
Boston University
110 Cummington St.
Boston, MA 02215

8. PERFORMING ORGANIZATION REPORT NUMBER

AM-97-022

9. SPONSORING / MONITORING AGENCY NAME(S) AND ADDRESS(ES)

U.S. Army Research Office
P.O. Box 12211
Research Triangle Park,, NC 27709-2211

10. SPONSORING / MONITORING AGENCY REPORT NUMBER

ARO 36216.1-EG

11. SUPPLEMENTARY NOTES

The views, opinions and/or findings contained in this report are those of the author(s) and should not be construed as an official Department of the Army position, policy or decision, unless so designated by other documentation.

12a. DISTRIBUTION / AVAILABILITY STATEMENT

Approved for public release; distribution unlimited.

12 b. DISTRIBUTION CODE

13. ABSTRACT *(Maximum 200 words)*

An entirely new approach to the large-eddy simulation (LES) of high-speed compressible turbulent flows is presented. Subgrid scale stress models are proposed that are dimensionless functions of the computational mesh size times a Reynolds stress model. This allows a DNS to go continuously to an LES and then a Reynolds-averaged Navier-Stokes (RANS) computation as the mesh becomes successively more coarse or the Reynolds number becomes much larger. Here, the level of discretization is parameterized by the non-dimensional ratio of the computational mesh size to the Kolmogorov length scale. The Reynolds stress model is based on a state-of-the-art two-equation model whose enhanced performance is documented in detail in a variety of benchmark flows. It contains many of the most recent advances in compressible turbulence modeling. Applications to the high-speed aerodynamic flows of technological importance are briefly discussed.

14. SUBJECT TERMS

Turbulence; Large-Eddy Simulations

15. NUMBER IF PAGES
31

16. PRICE CODE

17. SECURITY CLASSIFICATION OR REPORT	18. SECURITY CLASSIFICATION OF THIS PAGE	19. SECURITY CLASSIFICATION OF ABSTRACT	20. LIMITATION OF ABSTRACT
UNCLASSIFIED	UNCLASSIFIED	UNCLASSIFIED	UL

A COMBINED LARGE-EDDY SIMULATION AND TIME-DEPENDENT RANS CAPABILITY FOR HIGH-SPEED COMPRESSIBLE FLOWS

Charles G. Speziale

Aerospace & Mechanical Engineering Department

Boston University

Boston, MA 02215

ABSTRACT

An entirely new approach to the large-eddy simulation (LES) of high-speed compressible turbulent flows is presented. Subgrid scale stress models are proposed that are dimensionless functions of the computational mesh size times a Reynolds stress model. This allows a DNS to go continuously to an LES and then a Reynolds-averaged Navier-Stokes (RANS) computation as the mesh becomes successively more coarse or the Reynolds number becomes much larger. Here, the level of discretization is parameterized by the non-dimensional ratio of the computational mesh size to the Kolmogorov length scale. The Reynolds stress model is based on a state-of-the-art two-equation model whose enhanced performance is documented in detail in a variety of benchmark flows. It contains many of the most recent advances in compressible turbulence modeling. Applications to the high-speed aerodynamic flows of technological importance are briefly discussed.

1. INTRODUCTION

The high-speed turbulent flows of aerodynamic importance exhibit such a wide range of excited length and time scales that Direct Numerical Simulations (DNS) are all but impossible for the foreseeable future. These flows must invariably be computed based on some form of modeling. It has often been said that large-eddy simulations – where the large scales are computed directly while the small scales are modeled – are the most promising such approach (see Rogallo and Moin 1984 for an interesting review). However, as will be discussed in this paper, there are major problems with the way that traditional large-eddy simulations have been conducted. Furthermore, there is little experience with the large-eddy simulation of high-speed compressible turbulent flows (one of the few exceptions is the recent paper by Erlebacher, Hussaini, Speziale and Zang 1992). In addition, in practical wall-bounded turbulent flows, the Reynolds number can be so high (in many Naval applications it can be as large as 10^9) that the only feasible option is a RANS computation at this time. Hence, there is the need for a combined LES and RANS capability for compressible turbulent flows where the latter is of the time-dependent variety. This forms the motivation for the present paper.

Traditional large-eddy simulations have typically been based on the Smagorinsky (1963) model. The Smagorinsky model – along with its extensions such as the linear combination model (see Bardina, Ferziger and Reynolds 1983) – have the following two problems:

(1) The inability to respond to changes in the local state of the flow, causing the need to make *ad hoc* adjustments in the constants.

(2) The generally poor correlation with DNS at lower turbulence Reynolds numbers, even for simple benchmark cases.

As far as point (1) is concerned, turbulent channel flow, isotropic turbulence and more general, homogeneously strained turbulent flows all require different values of the Smagorinsky constant that can differ by more than a factor of two, even when given in its traditional form of $\sqrt{C_s}$ where C_s is the Smagorinsky constant. Furthermore, Van Driest wall damping has been needed which is empirical in nature and does not apply to general wall-bounded turbulent flows – particularly to those in complex geometries or with flow separation. Then, as

far as point (2) is concerned, even for the simple case of isotropic turbulence, the Smagorinsky model only correlates at the 50% level – an extremely poor result. It should be noted, for example, that the correlation between the functions $y = x$ and $y = e^{-x}$ on the interval [0, 1] is more than 60% despite the fact that they are qualitatively different functions (one is monotonically increasing while the other is a monotonically decreasing function)!

The only reason to believe that the Smagorinsky model is successful in these cases is probably due to the fact that it dissipates enough energy to roughly account for the cascade of energy to the scales that are left unresolved. With the desire to eliminate these problems, the dynamic subgrid scale model was recently developed (see Germano, Piomelli, Moin and Cabot 1991). In the dynamic subgrid scale model, a test filter is introduced in addition to the grid filter that is used in traditional LES. A variable Smagorinsky coefficient is then derived that depends on the local filtered rate-of-strain tensor as well as on the resolved turbulent stresses. The Smagorinsky coefficient then has the capability, in principle, of adapting automatically to the local state of the flow. While the dynamic subgrid scale model does contain many interesting new ideas, it, unfortunately, can further exacerbate the problem of contamination of the large scales by filtering and is not suitable for turbulent flows in complex geometries where the effect of the filter is never known with certainty and defiltering is not possible with any reliability. Furthermore, the dynamic subgrid scale model suffers from the same deficiency as the older subgrid scale models since, in the coarse mesh and infinite-Reynolds-number limit, a state-of-the-art Reynolds stress model is not recovered (the Smagorinsky model goes to a badly calibrated mixing length model in the coarse mesh limit). In the opinion of the author, future subgrid scale models must be theoretically based on a filter which does not significantly contaminate the large scales in so far as the model calibration is concerned – with the understanding that for complex turbulent flows one will never know precisely the effect of the filter and the filtered velocity must be used to approximate the large-scale part of the instaneous velocity for the calculation of turbulence statistics. In this manner, the issue of defiltering is completely avoided since it can never be done reliably anyhow (defiltering is equivalent to solving a Fredholm integral equation of the first kind which is mathematically ill-posed; see Hussaini, Speziale and Zang 1990). Then, even more importantly, a state-of-the-art Reynolds stress model should be recovered in the

coarse mesh/infinite-Reynolds-number limit. The dynamic subgrid scale model fails on both counts. Thus, new approaches must be tried.

An entirely new approach to compressible large-eddy simulations will be proposed in order to bridge the gap between LES and RANS. This new methodology will be based on state-of-the-art Reynolds stress models that incorporate many of the most recent developments in compressible turbulence modeling (see Speziale 1996). Subgrid scale models will be proposed that continuously go to Reynolds stress models in the coarse mesh/infinite Reynolds number limit. Furthermore, they automatically vanish in the fine mesh limit where a DNS is recovered. These points will be discussed in detail in the sections to follow and a variety of illustrative calculations will be provided.

2. THE COMPRESSIBLE REYNOLDS STRESS MODEL

In compressible turbulence, the velocity u_i, pressure p and absolute temperature T are solutions of the (cf. Cebeci and Smith 1974)

Navier-Stokes Equations

$$\frac{\partial}{\partial t}(\rho u_i) + (\rho u_i u_j)_{,j} = -p_{,i} - \frac{2}{3}(\mu u_{j,j})_{,i} + [\mu(u_{i,j} + u_{j,i})]_{,j} \tag{1}$$

Continuity Equation

$$\frac{\partial \rho}{\partial t} + (\rho u_i)_{,i} = 0 \tag{2}$$

Energy Equation

$$\frac{\partial}{\partial t}(\rho C_v T) + (\rho C_v u_i T)_{,i} = -p u_{i,i} + \Phi + (\kappa T_{,i})_{,i} \tag{3}$$

where the commonly used ideal gas equation of state is implemented in which

$$p = \rho R T.$$

Here, the viscous dissipation function

$$\Phi = \sigma_{i,j} u_{i,j} = -\frac{2}{3}\mu(u_{i,i})^2 + \mu(u_{i,j} + u_{j,i})u_{i,j}$$

and ρ is the mass density, R is the ideal gas constant, μ is the dynamic viscosity, C_v is the specific heat at constant volume, $\sigma_{ij} \equiv -\frac{2}{3}\mu u_{k,k}\delta_{ij} + \mu(u_{i,j} + u_{j,i})$ is the viscous stress tensor and κ is the thermal conductivity. In (1)–(3), the Einstein summation convention applies to repeated indices and $(\ \cdot\ )_{,i}$ denotes a gradient with respect to the spatial coordinates x_i.

Two alternative decompositions for the velocity field u_i, pressure p and temperature T into mean and fluctuating parts can be defined:

$$u_i = \overline{u}_i + u_i', \quad p = \overline{p} + p', \quad T = \overline{T} + T' \tag{4}$$

where an overbar represents a standard ensemble mean, and

$$u_i = \tilde{u}_i + u_i'', \quad p = \tilde{p} + p'', \quad T = \tilde{T} + T'' \tag{5}$$

where a tilde represents a Favre or mass weighted average defined as

$$\tilde{\mathcal{F}} = \frac{\overline{\rho \mathcal{F}}}{\overline{\rho}}$$

for any flow variable $\mathcal{F}$. A direct averaging of (1)–(3), yields the Reynolds-averaged Navier-Stokes, continuity and energy equations given by (cf. Cebeci and Smith 1974 and Speziale 1996):

Reynolds-Averaged Navier-Stokes Equations

$$\frac{\partial}{\partial t}(\overline{\rho}\tilde{u}_i) + (\overline{\rho}\tilde{u}_i\tilde{u}_j)_{,j} = -\overline{p}_{,i} - \frac{2}{3}(\overline{\mu u_{j,j}})_{,i} + \overline{[\mu(u_{i,j} + u_{j,i})]}_{,j} - (\overline{\rho}\tau_{ij})_{,j} \tag{6}$$

Reynolds-Averaged Continuity Equation

$$\frac{\partial \overline{\rho}}{\partial t} + (\overline{\rho}\tilde{u}_i)_{,i} = 0 \tag{7}$$

Reynolds-Averaged Energy Equation

$$\begin{aligned} \frac{\partial}{\partial t}(\overline{\rho}\overline{C}_v\tilde{T}) + (\rho\tilde{u}_i\overline{C}_v\tilde{T})_{,i} &= -\overline{p}\tilde{u}_{i,i} - \overline{p\widetilde{u''_{i,i}}} \\ -\overline{p'u'_{i,i}} + \overline{\Phi} + (\overline{\kappa T_{,i}})_{,i} - Q_{i,i} & \end{aligned} \tag{8}$$

where

$$\tau_{ij} \equiv \widetilde{u''_i u''_j}, \quad \overline{p} = \overline{\rho}R\tilde{T} \quad Q_i \equiv \overline{\rho}\overline{C_v}\widetilde{u''_i T''}$$

are the Favre-averaged Reynolds stress tensor, the ensemble averaged pressure and the Favre-averaged Reynolds heat flux where turbulent fluctuations in C_v have been neglected.

In high-Reynolds-number turbulent flows, the molecular diffusion terms are dominated by the turbulent transport terms except in a thin sublayer near walls. If we assume in this region that fluctuations in the viscosity, thermal conductivity and density can be neglected, we can then make the standard approximations (see Speziale 1996):

$$\begin{aligned} \overline{\sigma}_{ij} &\equiv -\frac{2}{3}\overline{\mu u_{k,k}}\delta_{ij} + \overline{\mu(u_{i,j} + u_{j,i})} \\ &\approx -\frac{2}{3}\overline{\mu}\tilde{u}_{k,k}\delta_{ij} + \overline{\mu}(\tilde{u}_{i,j} + \tilde{u}_{j,i}) \end{aligned} \tag{9}$$

$$\overline{q}_i \equiv -\overline{\kappa T_{,i}} \approx -\overline{\kappa}\tilde{T}_{,i}. \tag{10}$$

The mean viscous dissipation function is given by:

$$\begin{aligned} \overline{\Phi} &= \overline{\sigma}_{ij}\overline{u}_{i,j} + \overline{\sigma'_{ij}u'_{i,j}} \\ &= \overline{\sigma}_{ij}\tilde{u}_{i,j} + \overline{\sigma}_{ij}\overline{u''_{i,j}} + \overline{\rho}\varepsilon \end{aligned} \tag{11}$$

where $\varepsilon \equiv \overline{\sigma'_{ij} u'_{i,j}}/\overline{\rho}$ is the turbulent dissipation rate ($\overline{\Phi} \to \overline{\rho}\varepsilon$ as $Re \to \infty$). The pressure-dilatation correlation, mass flux and Reynolds heat flux are, respectively, modeled by (see Speziale 1996):

$$\overline{p' u'_{i,i}} = a_2 \overline{\rho} \tau_{ij} \tilde{u}_{i,j} M_t + a_3 \overline{\rho} \varepsilon M_t^2 \tag{12}$$

$$\overline{u''_i} = -\frac{\overline{\rho' u'_i}}{\overline{\rho}} \approx \frac{C_\mu}{\overline{\rho}\sigma_\rho} \frac{K^2}{\varepsilon} \overline{\rho}_{,i} \tag{13}$$

$$\widetilde{u''_i T''} \approx -\frac{C_\mu}{Pr_T} \frac{K^2}{\varepsilon} \tilde{T}_{,i} \tag{14}$$

where

$$C_\mu = 0.09, \quad \sigma_\rho = 0.5$$

$$Pr_T = 0.9, \quad a_2 = 0.15, \quad a_3 = 0.2.$$

and $M_t \equiv (2K/\gamma R\tilde{T})^{1/2}$ is the turbulent Mach number (see Speziale 1996, Speziale and Sarkar 1991 and Sarkar 1992). Here, Pr_T is the turbulent Prandtl number and $K \equiv \frac{1}{2}\tau_{ii}$ is the turbulent kinetic energy; $\gamma \equiv \overline{C}_p/\overline{C}_v$ is the ratio of mean specific heats at constant pressure and constant volume.

The Reynolds stress is represented by the explicit algebraic stress model (see Speziale 1996):

$$\begin{aligned} \tau_{ij} = {} & \frac{2}{3} K \delta_{ij} - \alpha_1^* \frac{K^2}{\varepsilon} (\tilde{S}_{ij} - \frac{1}{3} \tilde{S}_{kk} \delta_{ij}) - \alpha_2^* \frac{K^3}{\varepsilon^2} (\tilde{S}_{ik} \tilde{\omega}_{kj} \\ & + \tilde{S}_{jk} \tilde{\omega}_{ki}) + \alpha_3^* \frac{K^3}{\varepsilon^2} \left(\tilde{S}_{ik} \tilde{S}_{kj} - \frac{1}{3} \tilde{S}_{kl} \tilde{S}_{kl} \delta_{ij} \right) \end{aligned} \tag{15}$$

where

$$\alpha_i^* = \alpha_i \left(\frac{3}{3 - 2\eta^2 + 6\xi^2} \right) \tag{16}$$

for $i = 1, 2, 3$ and

$$\alpha_1 = \left(\frac{4}{3} - C_2 \right) g, \quad \alpha_2 = \frac{1}{2} \left(\frac{4}{3} - C_2 \right) (2 - C_4) g^2$$

$$\alpha_3 = \left(\frac{4}{3} - C_2 \right) (2 - C_3) g^2, \quad g = \left(\frac{1}{2} C_1 + \frac{\mathcal{P}}{\varepsilon} - 1 \right)^{-1}$$

$$\eta = \frac{1}{2} \frac{\alpha_3}{\alpha_1} \frac{K}{\varepsilon} (\tilde{S}_{ij} \tilde{S}_{ij})^{1/2}, \; \xi = \frac{\alpha_2}{\alpha_1} \frac{K}{\varepsilon} (\tilde{\omega}_{ij} \tilde{\omega}_{ij})^{1/2}. \tag{17}$$

This explicit algebraic stress model – which is in the form of an anisotropic eddy viscosity

model with strain-dependent coefficients – is obtained from the explicit solution of the equilibrium form of the modeled Reynolds stress transport equation for incompressible turbulent flows (see Gatski and Speziale 1993). It is then extended to compressible flows. In (17), $\mathcal{P}/\varepsilon$ is set to one and $C_1 - C_4$ are constants that assume the values of 5.20, 0.36, 1.25 and 0.40, respectively. Here, again the turbulent kinetic energy $K \equiv \frac{1}{2}\tau_{ii}$. For general turbulent flows, α_i^* is represented by the regularized expressions

$$\alpha_1^* = \frac{(1+2\xi^2)(1+6\eta^5)+\frac{5}{3}\eta^2}{(1+2\xi^2)(1+2\xi^2+\eta^2+6\beta_1\eta^6)}\alpha_1 \tag{18}$$

$$\alpha_i^* = \frac{(1+2\xi^2)(1+\eta^4)+\frac{2}{3}\eta^2}{(1+2\xi^2)(1+2\xi^2+\beta_i\eta^6)}\alpha_i \tag{19}$$

for $i = 2, 3$ where

$$\beta_1 = 7.0, \quad \beta_2 = 6.3, \quad \beta_3 = 4.0.$$

This is obtained by a Pade' approximation which builds in some limited agreement with Rapid Distortion Theory (RDT) (see Speziale and Xu 1996).

The turbulent kinetic energy is a solution of the transport equation:

$$\begin{aligned} \frac{\partial}{\partial t}(\overline{\rho}K) + (\overline{\rho}\tilde{u}_i K)_{,i} &= -\overline{\rho}\tau_{ij}\tilde{u}_{i,j} - \overline{\rho}\varepsilon \\ &\quad + \overline{p'u'_{i,i}} - \overline{u''_i}\overline{p}_{,i} + \overline{u''_i}\overline{\sigma}_{ij,j} \\ &\quad + \left[\left(\overline{\mu} + \frac{\overline{\mu}_T}{\sigma_k}\right)K_{,i}\right]_{,i} \end{aligned} \tag{20}$$

where

$$\overline{\mu}_T = C_\mu \overline{\rho}\frac{K^2}{\varepsilon}$$

is the eddy viscosity and $C_\mu \approx 0.09$ is taken to be a constant; σ_k is a constant equal to one. The dissipation rate equation takes the compressible modeled form (see Speziale 1996):

$$\begin{aligned} \frac{\partial}{\partial t}(\overline{\rho}\varepsilon) + (\overline{\rho}\tilde{u}_i\varepsilon)_{,i} &= -C_{\varepsilon 1}\overline{\rho}\frac{\varepsilon}{K}\tau_{ij}\left(\tilde{u}_{i,j} - \frac{1}{3}\tilde{u}_{k,k}\delta_{ij}\right) \\ &\quad - \frac{4}{3}\overline{\rho}\varepsilon\tilde{u}_{i,i} + C_{\varepsilon 3}R_t{}^{1/2}\frac{\varepsilon^2}{K} - C_{\varepsilon 2}\overline{\rho}\frac{\varepsilon^2}{K} \\ &\quad + \left[\left(\overline{\mu} + \frac{\overline{\mu}_T}{\sigma_\varepsilon}\right)\varepsilon_{,i}\right]_{,i} \end{aligned} \tag{21}$$

where σ_ε is a constant that assumes the value of approximately 1.3 and $C_{\varepsilon 1} = 1.44$, $C_{\varepsilon 2} = 1.83$ and $C_{\varepsilon 3} = 0.001$; $R_t \equiv K^2/\overline{\nu}\varepsilon$ is the turbulence Reynolds number. This dissipation rate model can be directly integrated to a solid boundary with no wall damping (see Speziale and Abid 1995). Only the singularity need be removed in the destruction term where a simple modification in $C_{\varepsilon 2}$ is made. The vortex stretching term in the expression containing $C_{\varepsilon 3}$ leads to a better behaved model without compromising the predictions in benchmark equilibrium turbulent flows. For example, it removes the singularity in plane stagnation point turbulent flows (see Abid and Speziale 1996). Furthermore, it allows a universal equilibrium value of $\mathcal{P}/\varepsilon = 1$ to be used in the explicit algebraic stress models with good agreement for both homogeneous shear flow and the log-layer. Setting $\mathcal{P}/\varepsilon$ to a constant makes the model more robust. The Sarkar compressible dissipation model (see Sarkar *et al.* 1991 and Zeman 1990) was not implemented because it is either negligible or does not do well in the log-layer and it is our purpose to develop a model suitable for supersonic wall-bounded turbulent flows.

3. A NEW APPROACH TO LARGE-EDDY SIMULATIONS

In the large-eddy simulation of compressible turbulent flows the filtered equations of motion are given by:

Filtered Navier-Stokes Equations

$$\frac{\partial}{\partial t}(\overline{\rho}\tilde{u}_i) + (\overline{\rho}\tilde{u}_i\tilde{u}_j)_{,j} = -\overline{p}_{,i} - \frac{2}{3}(\overline{\mu}\tilde{u}_{j,j})_{,i} + [\overline{\mu}(\tilde{u}_{i,j} + \tilde{u}_{j,i})]_{,j} - (\overline{\rho}\tau_{ij}^S)_{,j} \tag{22}$$

Filtered Continuity Equation

$$\frac{\partial \overline{\rho}}{\partial t} + (\overline{\rho}\tilde{u}_i)_{,i} = 0 \tag{23}$$

Filtered Energy Equation

$$\frac{\partial}{\partial t}(\overline{\rho}\overline{C}_v\tilde{T}) + (\rho\tilde{u}_i\overline{C}_v\tilde{T})_{,i} = -\overline{p}\tilde{u}_{i,i} - \overline{p}(\overline{u_{i,i}''})^S$$

$$-(\overline{p'u_{i,i}'})^S + \overline{\Phi}^S + (\overline{\kappa}\tilde{T}_{,i})_{,i} - Q_{i,i}^S \tag{24}$$

where $\tau_{ij}^S, (u_i'')^S, (\overline{p'u_{i,i}'})^S, \overline{\Phi}^S$ and Q_i^S are, respectively, the subgrid scale Reynolds stress tensor, the subgrid scale mass flux, the subgrid scale pressure-dilatation correlation, the subgrid scale dissipation function and the subgrid sca le Reynolds heat flux. The approximations discussed in the previous section for the diffusion terms in (9)–(10) were made. It should be noted that the filtered equations of motion are *identical* in form to the Reynolds-averaged equations of motion discussed earlier. This will allow us to develop a combined LES and time-dependent RANS capability. In (22)–(24) an overbar represents a standard filter and a tilde represents a Favre filter. For any flow variable $\mathcal{F}$ they are defined as follows:

$$\overline{\mathcal{F}} = \int_D G(\mathbf{x} - \mathbf{x}^*, \Delta)\mathcal{F}(\mathbf{x}^*)d^3x^* \tag{25}$$

where G is a filter function, Δ is the computational mesh size and

$$\tilde{\mathcal{F}} = \frac{\overline{\rho\mathcal{F}}}{\overline{\rho}}.$$

A compact filter of bounded support, such as the box filter, can be implemented in complex geometries where

$$G(\mathbf{x} - \mathbf{x}^*, \Delta) = \begin{cases} 1/8\Delta^3, & |x_i - x_i^*| \leq \Delta \\ 0, & |x_i - x_i^*| > \Delta \end{cases} \tag{26}$$

for $i = 1, 2, 3$ (cf. Leonard 1974 and Ferziger 1976).

Models for the subgrid scale stress tensor τ_{ij}^S are proposed that are of the form:

$$\tau_{ij}^S = [1 - exp(-\beta\Delta/L_K)]^n \tau_{ij} \tag{27}$$

where τ_{ij} is a Reynolds stress model, Δ is the computational mesh size, L_K is the Kolmogorov length scale, and β and n are constants. In the Reynolds stress model, the ensemble averages are taken to be filtered quantities (in complex geometries we never know the effect of the filter anyhow). In the limit as $\Delta/L_K \rightarrow 0$, all relevant scales are resolved and we have a direct simulation where $\tau_{ij} = 0$; as $\Delta/L_K \rightarrow \infty$ and the mesh becomes coarse or the Reynolds number becomes extremely large, we recover a Reynolds stress model and a RANS computation. In between these two limits, we have an LES or a VLES (the latter denotes a large-eddy simulation where the preponderance of the turbulent kinetic energy is unresolved). Here, it should be noted that in the simulation of turbulence, the computational mesh is fine (or coarse) depending on whether Δ is small (or large) compared to the Kolmogorov length scale $L_K \equiv \overline{\nu}^{3/4}/\varepsilon^{1/4}$ where $\overline{\nu} \equiv \overline{\mu}/\overline{\rho}$. This automatically brings in a dependence on the turbulence Reynolds number R_t ($R_t \equiv K^2/\overline{\nu}\varepsilon$) since $L_K = R_t^{-3/4} K^{3/2}/\varepsilon$. An estimate of the Kolmogorov length scale is provided by the modeled transport equation for ε discussed earlier. In order to estimate the the Kolmogorov length scale to within 10% it is only required that the dissipation rate be estimated to within 50% since the dissipation rate is raised to the 1/4 power. Hence, it is quite reasonable to expect that an acceptable estimate of the Kolmogorov length scale can be obtained (this is a crucial element of this proposed approach). The Reynolds stress model in (27) is represented by the expressions discussed in Section 2. It was recently shown by Speziale and Abid 1995 that this type of two-equation model can be integrated directly to a solid boundary with no wall damping functions; only the singularity in the ε – transport equation needs to be removed.

Initially we have chosen

$$\beta \approx 0.001, \quad n = 1.$$

Hence, for $\Delta/L_K < 10$ – which is a value encountered in many practical LES – the grid function in (27) can be approximated by a power law. Interestingly enough, Woodruff and Hussaini (*Private Communication*) have arrived at a power law representation for the grid

function in (27) via Renormalization Group techniques. This shows that there is some theoretical basis for this idea.

The same modeling technique is implemented for the subgrid scale mass flux, subgrid scale pressure-dilatation correlation, subgrid scale dissipation function and subgrid scale Reynolds heat flux. More specifically, subgrid scale models are implemented which are of the form

$$(u_i'')^S = [1 - exp(-\beta\Delta/L_K)]^n u_i'' \tag{28}$$

$$(\overline{p'u_{i,i}'})^S = [1 - exp(-\beta\Delta/L_K)]^n \overline{p'u_{i,i}'} \tag{29}$$

$$\overline{\Phi}^S = [1 - exp(-\beta\Delta/L_K)]^n \overline{\Phi} \tag{30}$$

$$Q_i^S = [1 - exp(-\beta\Delta/L_K)]^n Q_i \tag{31}$$

where the mass flux, pressure-dilatation correlation, dissipation function and Reynolds heat flux on the right-hand-side of (28)–(31) are modeled in the Reynolds-averaged forms provided in Section 2. However, an overbar or tilde is taken to be a standard or Favre filter, respectively. For the practical LES of high Reynolds number turbulent flows, the subgrid scale mass flux and subgrid scale pressure-dilatation correlation can be neglected (see Erlebacher, Hussaini, Speziale and Zang 1992). Furthermore, the mean dissipation function can be approximated by $\overline{\Phi} \approx \overline{\rho}\varepsilon$ which leads to a considerable simplification.

Some comments are needed concerning the choice of a filter in this new approach to large-eddy simulations. We want a filter that yields the minimum contamination of the large scales. The reason for this is clear; defiltering must be avoided since it constitutes an ill-posed mathematical problem as stated earlier. The main purpose of practical LES is to predict the Reynolds-averaged fields. In order to do so, the filtered velocity must invariably be used to estimate the instaneous velocity which then yields the Reynolds-averaged fields through appropriate ensemble averages. Here, the large scales make the dominant contribution to the most pertinent fields such as the turbulent kinetic energy. A minimum contamination of the large scales can be accomplished with, of the order of, a 128^3 computational mesh using a filter with a compact support – such as the box filter – which has a small filter width of, say, two mesh points. Some of the previously conducted coarse grid LES (which has typically had no more than 32^3 mesh points) must be avoided wherein the filter width has,

at times, been as much as 25% of the computational domain, significantly contaminating the large scales. Besides, recent increases in computational capacity have begun to make 128^3 computations much more feasible for engineering calculations (a small compromise to 100^3 computations can always be made). In addition, it should be noted that practical LES – in complex geometries – will require the use of finite difference techniques with a compact filter (these should be based on fourth-order accurate finite difference schemes). Some illustrative calculations will be provided in the next Section to demonstrate the potential of this new approach for practical engineering calculations.

4. ILLUSTRATIVE CALCULATIONS

First, we will present some results for incompressible flows to demonstrate that the model behaves correctly in the limit of small Mach numbers. As mentioned earlier, this two-equation model can be integrated directly to a solid boundary with no wall damping. Results were obtained for the incompressible flat plate boundary layer at zero pressure gradient. In Figure 1, the skin friction coefficient obtained from this model – plotted as function of the Reynolds number based on the momentum thickness, R_θ – is compared with experimental data (see Wieghardt and Tillman 1951) and with results obtained from the $K-\varepsilon$ model with wall damping (see Speziale, Abid and Anderson 1992). Clearly, the results are extremely good. No wall damping functions are needed; the singularity which occurs at the wall only needs to be removed from the dissipation rate equation (see Speziale and Abid 1995). The fact that excellent predictions for the Reynolds stresses are obtained starting in the log-layer is demonstrated in Figure 2 where the turbulence intensities are depicted. A Reynolds stress model cannot be expected to accurately describe the turbulence structure immediately adjacent to a wall since it exhibits such a wide range of scales and diverse turbulence physics. We only need to have Reynolds stress models that can operationally be integrated to a wall without compromising their predictive capabilities away from the wall. This can be accomplished with the model discussed herein.

In Figure 3, the prediction of this two-equation model for the mean velocity profile in rotating channel flow is compared with the experimental data of Johnston, Halleen and Lezius (1972) for a rotation number $Ro = 0.068$. It is clear from these results that the model correctly predicts that the mean velocity profile is *asymmetric* in line with the experimental results – an effect that arises from Coriolis forces. In contrast to these results, the standard $K-\varepsilon$ model incorrectly predicts a symmetric mean velocity profile identical to that obtained in an inertial frame (the standard $K-\varepsilon$ model is oblivious to rotations of the reference frame). As demonstrated by Gatski and Speziale (1993), the results obtained in Figure 3 with this two-equation model are virtually as good as those obtained from a full second-order closure. This is due to the fact that a representation is used for the Reynolds stress tensor that is a two-equation model which is formally derived from a second-order closure in the equilibrium limit. It is now clear that previous claims that two-equation models cannot systematically

account for rotational effects were erroneous.

A few examples will now be presented that illustrate the enhanced predictions that are obtained for turbulent flows exhibiting effects arising from normal Reynolds stress differences. Here, we will show results obtained from the nonlinear $K-\varepsilon$ model of Speziale (1987) (also see Yoshizawa 1984). For turbulent shear flows that are predominantly unidirectional, with secondary flows or recirculation zones driven by small normal Reynolds stress differences, a quadratic approximation to the anisotropic eddy viscosity model described herein collapses to the nonlinear $K-\varepsilon$ model (see Gatski and Speziale 1993). In Figure 4, it is demonstrated that the nonlinear $K-\varepsilon$ model predicts an eight-vortex secondary flow, in a square duct, in line with experimental observations; on the other hand, the standard $K-\varepsilon$ model erroneously predicts that there is no secondary flow. In order to be able to predict secondary flows in non-circular ducts, the axial mean velocity $\overline{u}_z$ must give rise to a non-zero normal Reynolds stress difference $\tau_{yy}-\tau_{xx}$. This requires an *anisotropic* eddy viscosity (any isotropic eddy viscosity, including that used in the standard $K-\varepsilon$ model, yields a vanishing normal Reynolds stress difference which makes it impossible to describe these secondary flows).

In Figure 5, results obtained from the nonlinear $K-\varepsilon$ model are compared with the experimental data of Kim, Kline and Johnston (1980) and Eaton and Johnston (1980) for turbulent flow past a backward facing step. It is clear that these results are excellent: reattachment is predicted at $x/H \approx 7.0$ in close agreement with the experimental data (see Figure 5(a)). The Reynolds shear stresses are also well represented by the model (see Figure 5(b)). In contrast to these results, the standard $K-\varepsilon$ model predicts reattachment at $x/H \approx 6.25$ – an 11% underprediction. This error predominantly results from the inaccurate prediction of normal Reynolds stress anisotropies in the recirculation zone as discussed by Speziale and Ngo (1988).

The basic two-equation model discussed herein has recently been shown to be feasible for complex aerodynamic computations by Abid, Morrison, Gatski and Speziale (1996) in the compressible regime (the transonic flow regime to be specific). The ONERA M6 wing at a Mach number of $M_\infty = 0.8447$ with an angle of attack of $\alpha = 5.06^o$ and a Reynolds number of $Re = 11.7 \text{ x } 10^6$ has been considered. At this Mach number the turbulence statistics behave quasi-incompressibly (compressibility effects are primarily felt through changes in the mean

density since the Morkovin hypothesis applies). In Figure 6, a comparison is made of the computed surface pressure distributions with experiments (see Schmitt and Charpin 1979) at four different spanwise locations. As can be seen, the results are quite good. They are shown primarily to establish the feasibility of this new two-equation model for the calculation of complex compressible flows.

Some preliminary LES results will now be provided for the developing incompressible turbulent boundary layer at zero pressure gradient — integrated through transition. These computations were conducted by H. Fasel and his group at the University of Arizona using an empirically based ramp function — that depends explicitly on the momentum thickness Reynolds number and the mesh size with a simple eddy viscosity model — as a preliminary test of the ideas embodied in (27). In Figure 7, the spanwise vorticity obtained from the LES is shown which compares favorably with the corresponding results obtained from DNS. It is clear that the subgrid scale model allows the LES to pick up the pertinent flow structures and to be integrated through transition (laminar - turbulent flow). The ramp function, which forms a central part of (27), allows the eddy viscosity to gradually turn on as the flow becomes turbulent. In this regard, the corresponding eddy viscosity is displayed in Figure 8. These calculations - which have yielded encouraging results - are being repeated for the compressible turbulent boundary layer.

Unlike in many existing dissipation rate models, the dilatational part of the production terms in (21) are consistent with rapid distortion theory for compressible isotropic turbulence. For the problem of a rapid compression or expansion of isotropic turbulence, the mean velocity gradient tensor is given by

$$\tilde{u}_{i,j} = \begin{pmatrix} \frac{1}{3}\Gamma & 0 & 0 \\ 0 & \frac{1}{3}\Gamma & 0 \\ 0 & 0 & \frac{1}{3}\Gamma \end{pmatrix} \tag{32}$$

where Γ is the expansion/compression rate which is constant. The two-equation model provided herein reduces, in this case, approximately to the simple system of coupled ODE's:

$$\dot{K} = -\frac{2}{3}\Gamma K \tag{33}$$

$$\dot{\varepsilon} = -\frac{4}{3}\Gamma \varepsilon \tag{34}$$

for $|\Gamma|K_0/\varepsilon_0 \gg 1$. The short-time solution to Eqs. (33) - (34) is given by:

$$K = K_0 \exp\left(-\frac{2}{3}\Gamma t\right) \tag{35}$$

$$\varepsilon = \varepsilon_0 \exp\left(-\frac{4}{3}\Gamma t\right) \tag{36}$$

$$\Lambda = \Lambda_0 \exp\left(\frac{1}{3}\Gamma t\right) \tag{37}$$

where $\Lambda \equiv K^{3/2}/\varepsilon$ is the integral length scale. *This solution is essentially identical to the results obtained by Reynolds (1987) based on Rapid Distortion Theory (RDT).* In contrast to these results, a variable density extension of the commonly used second-order closures erroneously predicts that

$$\Lambda = \Lambda_0 \exp(-0.04\Gamma t) \tag{38}$$

(see Reynolds 1987). According to (38), the integral length scale will *decrease* under an expansion ($\Gamma > 0$) and *increase* under a compression ($\Gamma < 0$) – results that are clearly in error as first pointed out by Reynolds (1987). It is believed that this correction will lead to a better behaved model in regions of strong straining which can occur when shock waves are present.

Interesting enough, *good results are obtained for the compressible flat plate boundary layer with this two-equation model for Mach numbers M_∞ as large as* 8 *and wall temperature ratios as low as* 0.3 with *no* explicit dilatation terms, as first calculated by Zhang *et al.* (1993) (see Figure 9). In fact, it must be noted that the compressible dissipation model of Sarkar causes a degradation of the skin friction predictions; the model is not formally correct in the log-layer of high-speed compressible boundary layers. This was probably first pointed out by P. G. Huang (see Huang *et al.* 1994). That is why we have chosen to exclude the compressible or dilatational dissipation from the model. It is not needed to get good results in the compressible turbulent boundary layer and we are interested in describing high-speed compressible wall-bounded flows.

5. CONCLUSION

A new combined LES and time-dependent RANS capability for the computation of the high-speed compressible turbulent flows of technological importance has been proposed. In this new methodology, subgrid scale models go continuously to Reynolds stress models in the coarse mesh/infinite Reynolds number limit. Here, it is believed that in complex wall-bounded turbulent flows – especially with flow separation where wall functions cannot be used – the best that one can do, at this time, for the extremely high Reynolds numbers encountered in many technological applications (such as some naval flows where $Re \sim O(10^9)$) is a RANS computation since the crucial wall layer cannot be resolved. At more moderate Reynolds numbers, LES is possible (of course at extremely low turbulence Reynolds numbers it is possible to conduct a DNS). The RANS model that was presented in this study is a two-equation model that contains some of the most recent developments in compressible turbulence modeling. In the incompressible limit it collapses to an explicit algebraic stress model which is a two-equation model that is consistent with a state-of-the-art second-order closure model in the limit of homogeneous turbulence in equilibrium. A mild non-equilibrium extension is then built in via a Pade' approximation that has some limited agreement with Rapid Distortion Theory (RDT). The performance of this two-equation model was documented in a variety of benchmark turbulent flows. This performance was surprisingly good.

A few words are warranted concerning supersonic turbulent flows – particularly in wall-bounded geometries. Since there is considerable heating in such flows, the effective Reynolds number (through a rise in the kinematic viscosity) is not extremely large even in many of the high-speed compressible flows of technological importance. Thus, the prospects for being able to conduct a large-eddy simulation in many practical flow situations are fairly good for compressible turbulence. This would include the flow around high-speed aircraft and missiles to name just a few applications. For those cases where LES is not feasible, a time-dependent RANS can be always be conducted which is expected to be far superior to traditional steady RANS. The methodology discussed in this paper has the potential to make a significant impact on such problems in each of these dual areas. Preliminary results are quite promising and further tests are currently underway.

ACKNOWLEDGEMENTS

This work was supported by the Army Research Office under Contract No. DAAG55-97-1-0123, Dr. T. Doligalski, Project Monitor. The author is indebted to Prof. H. Fasel (University of Arizona) for providing his LES results of the turbulent boundary and for his collaborations.

REFERENCES

Abid, R. and Speziale, C. G., 1996. "The freestream matching condition for stagnation point turbulent flows: An alternative formulation," *ASME J. Appl. Mech.* **63**, pp. 95-100.

Abid, R., Morrison, J. H., Gatski, T. B. and Speziale, C. G., 1996. "Prediction of aerodynamic flows with a new explicit algebraic stress model," *AIAA Journal* **34**, pp. 2632–2635.

Bardina, J., Ferziger, J. H. and Reynolds, W. C., 1983. "Improved turbulence models based on large-eddy simulation of homogeneous, incompressible turbulent flows," *Stanford University Technical Report No. TF-19.*

Cebeci, T. and Smith, A. M. O., 1974. *Analysis of Turbulent Boundary Layers*, Academic Press, New York.

Eaton, J. K. and Johnston, J. P., 1980. "Turbulent flow reattachment: An experimental study of the flow and structure behind a backward facing step," *Stanford University Report No. MD-39.*

Erlebacher, G., Hussaini, M. Y., Speziale, C. G. and Zang, T. A., 1992. "Toward the large-eddy simulation of compressible turbulent flows", *J. Fluid Mech.* **238**, pp. 155-185.

Ferziger, J. H., 1976. "Large-eddy simulation of turbulent flows," *AIAA Paper No. 76-347.*

Gatski, T. B. and Speziale, C. G., 1993. "On explicit algebraic stress models for complex turbulent flows," *J. Fluid Mech.* **254**, pp. 59-78.

Germano, M., Piomelli, U., Moin, P. and Cabot, W. H., 1991. "A dynamic subgrid-scale eddy viscosity model," *Phys. Fluids* **3**, pp. 1760-1765.

Huang, P. G., Bradshaw, P. and Coakley, T. J., 1994. "Turbulence models for compressible boundary layers," *AIAA J.* **32**, pp. 735-740.

Hussaini, M. Y., Speziale, C. G. and Zang, T. A., 1990. "Discussion of the potential and limitations of direct and large-eddy simulations," *Lecture Notes in Physics* **357**, pp. 354-368.

Johnston, J. P., Halleen, R. M. and Lezius, D. K., 1972. "Effects of a spanwise rotation on the structure of two-dimensional fully-developed turbulent channel flow," *J. Fluid Mech.* **56**, pp. 533-557.

Kim, J., Kline, S. J. and Johnston, J. P., 1980. "Investigation of a reattaching turbulent shear layer: Flow over a backward facing step," *ASME J. Fluids Eng.* **102**, pp. 302-308.

Kussoy, M. I. and Horstman, C. C., 1991. "Documentation of two- and three-dimensional shock wave/turbulent boundary layer interaction flows at Mach 8.2," *NASA TM-103838.*

Leonard, A., 1974. "On the energy cascade in large-eddy simulations of turbulent flows," *Adv. Geophys. A* **18**, pp. 237-248.

Reynolds, W. C., 1987. "Fundamentals of turbulence for turbulence modeling and simulation," in *Lecture Notes for Von Kármán Institute, AGARD Lect. Ser. No.* 86, pp. 1-66, NATO, New York.

Rogallo, R. S. and Moin, P., 1984. "Numerical simulation of turbulent flows," *Ann. Rev. Fluid Mech* **16**, pp. 99-137.

Sarkar, S., 1992. "The pressure-dilatation correlation in compressible flows," *Phys. Fluids A* **4**, pp. 2674-2682.

Sarkar, S., Erlebacher, G. and Hussaini, M. Y., 1991. "Direct simulation of compressible turbulence in a shear flow," *Theor. & Comp. Fluid Dyn.* **2**, pp. 291-305.

Schmitt, V. and Charpin, F., 1979. "Pressure distribution on the ONERA M6 wing at transonic Mach numbers," *AGARD-AR-138*, NATO, New York.

Smagorinsky, J., 1963. "General circulation experiments with the primitive equations," *Mon. Weather Review* **91**, pp. 99-165.

Speziale, C. G., 1987. "On nonlinear $K - \ell$ and $K - \varepsilon$ models of turbulence," *J. Fluid Mech.* **178**, pp. 459-475.

Speziale, C. G., 1996. "Modeling of Turbulent Transport Equations," in *Simulation and Modeling of Turbulent Flows*, (T. B. Gatski, M. Y. Hussaini and J. L. Lumley, eds.), pp. 185-242, Oxford Univ. Press, New York.

Speziale, C. G. and Abid, R., 1995. "Near-wall integration of Reynolds stress turbulence closures with no wall damping," *AIAA J.* **33**, pp. 1974-1977.

Speziale, C. G. and Ngo, T., 1988. "Numerical solution of turbulent flow past a backward facing step using a nonlinear $K - \varepsilon$ model," *Int. J. Eng. Sci.* **26**, pp. 1099-1112.

Speziale, C. G. and Sarkar, S., 1991. "Second-order closure models for supersonic turbulent flows," *AIAA Paper No. 91-0217.*

Speziale, C. G. and Xu, X. H., 1996. "Towards the development of second-order closure models for non-equilibrium turbulent flows," *Int. J. Heat & Fluid Flow* **17**, pp. 238-244.

Speziale, C. G., Abid, R. and Anderson, E. C., 1992. "Critical evaluation of two-equation models for near-wall turbulence," *AIAA J.*, **30**, pp. 324-331.

Wieghardt, K. and Tillman, W., 1951. "On the turbulent friction layer for rising pressure," *NACA TM 1314.*

Yoshizawa, A., 1984. "Statistical analysis of the deviation of the Reynolds stress from its eddy viscosity representation," *Phys. Fluids* **27**, pp. 1377-1387.

Zeman, O., 1990. "Dilatational dissipation: The concept and application in modeling compressible mixing layers," *Phys. Fluids A* **2**, pp. 178-188.

Zhang, H. S., So, R. M. C., Speziale, C. G. and Lai, Y. G., 1993. "Near-wall two-equation model for compressible turbulent flows," *AIAA J.* **31**, pp. 196-199.

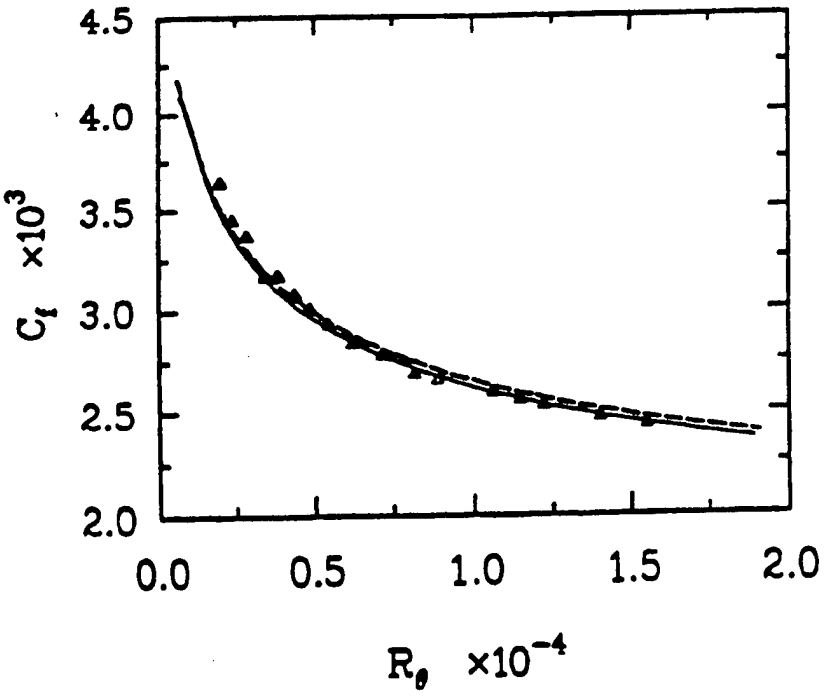

Figure 1. Comparison of the predictions of the proposed two-equation model for skin friction with experimental data (Wieghardt and Tillman 1951) for the incompressible flat plate turbulent boundary layer.

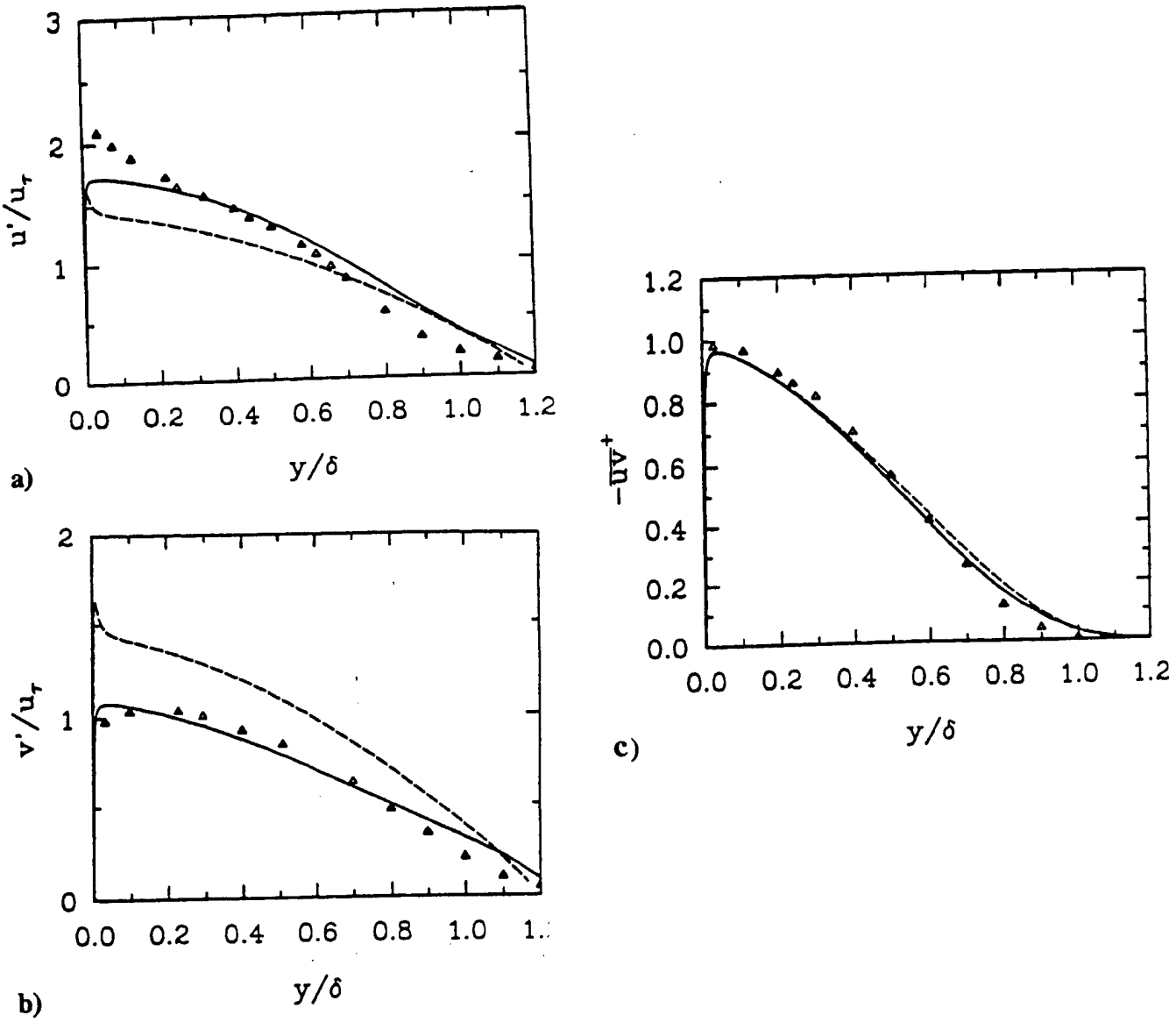

Figure 2. Incompressible turbulent flat plate boundary layer: Comparison of the predictions of the (——) proposed two-equation model and the (- - -) Speziale, Abid and Anderson (1992) model with (△) experimental data (Wieghardt and Tillman 1951). (a) Streamwise turbulence intensity, (b) turbulence intensity normal to wall and (c) turbulent shear stress.

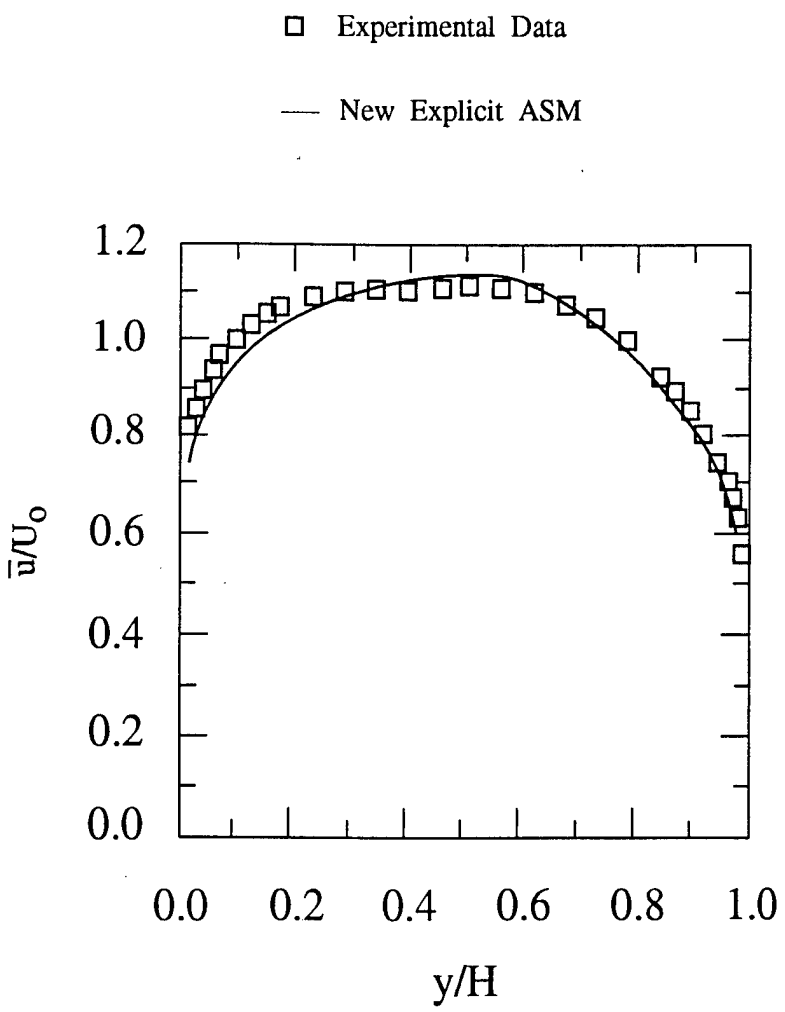

Figure 3. Comparison of the mean velocity profile in incompressible rotating channel flow predicted by the proposed two-equation model with the experimental data of Johnston, Halleen and Lezius (1972).

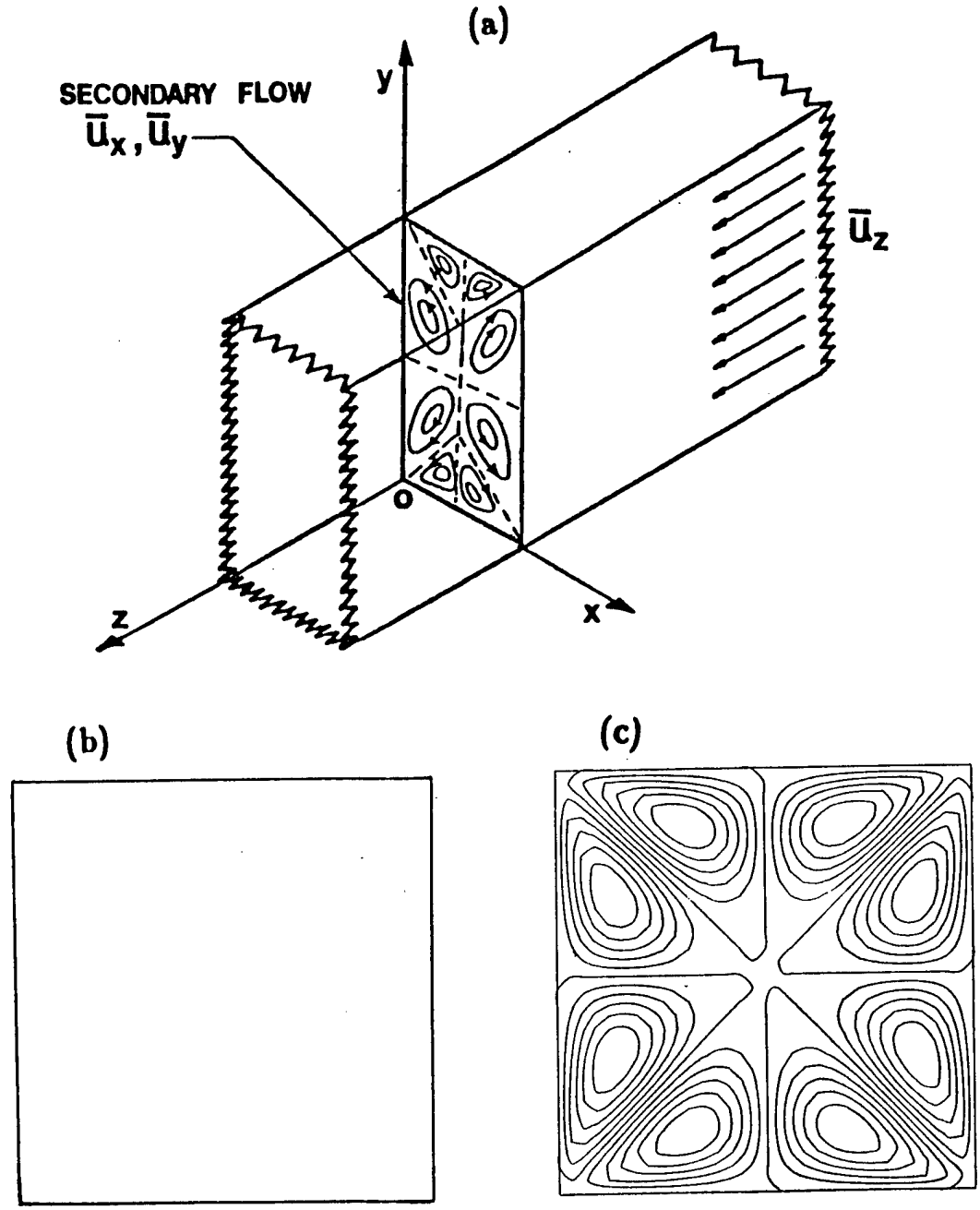

Figure 4. Incompressible turbulent secondary flow in a rectangular duct: (a) experiments, (b) standard $K - \varepsilon$ model, and (c) nonlinear $K - \varepsilon$ model of Speziale (1987).

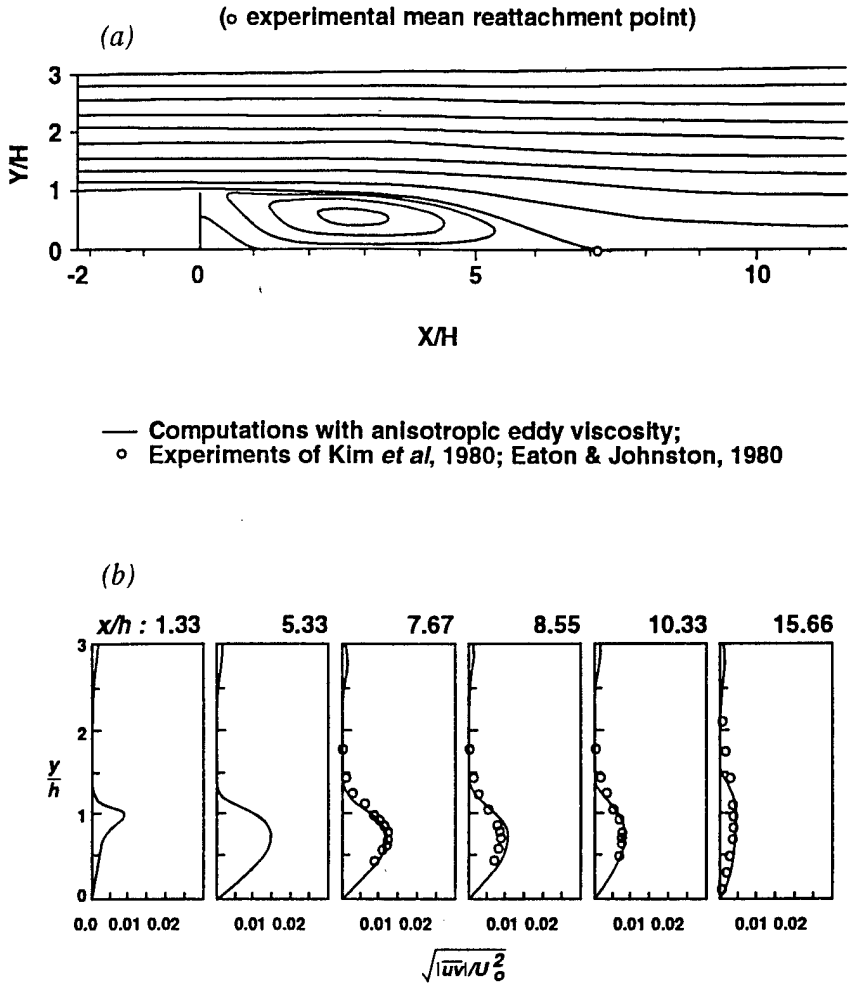

Figure 5. Incompressible turbulent flow past a backward facing step: comparison of the predictions of the nonlinear $K-\varepsilon$ model of Speziale (1987) with experiments. (a) Streamlines and (b) turbulent shear stress profiles.

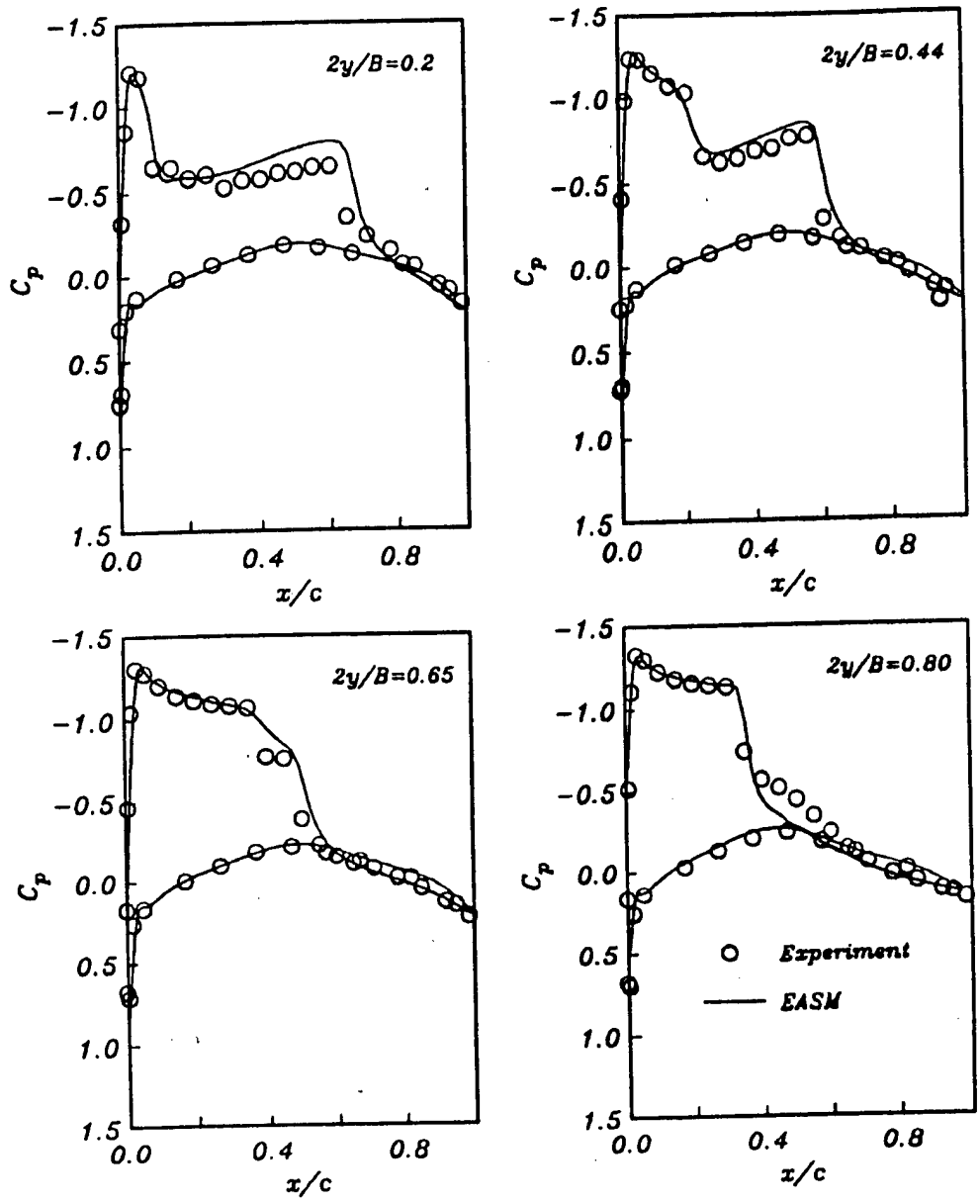

Figure 6. Compressible surface pressure distributions for the ONERA M6 wing at four different spanwise locations predicted by the proposed two-equation model (—). Experiments of Schmitt and Charpin (1979) denoted by (o).

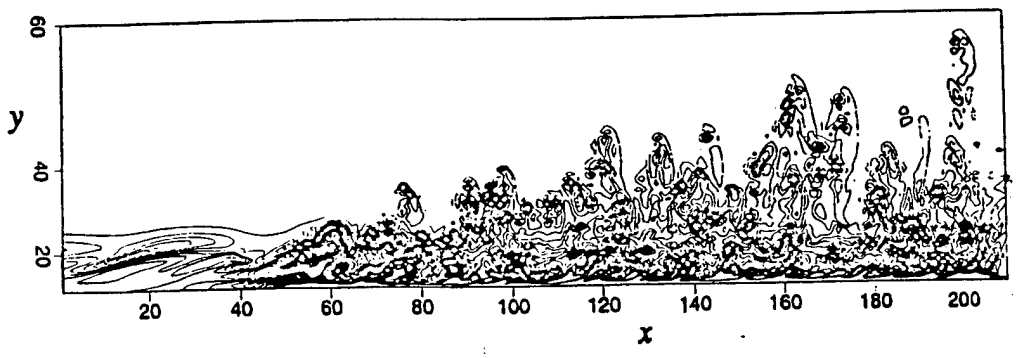

Figure 7. Plot of spanwise vorticity in the developing incompressible turbulent boundary layer obtained from LES (computations done by H. Fasel and co-workers at the University of Arizona).

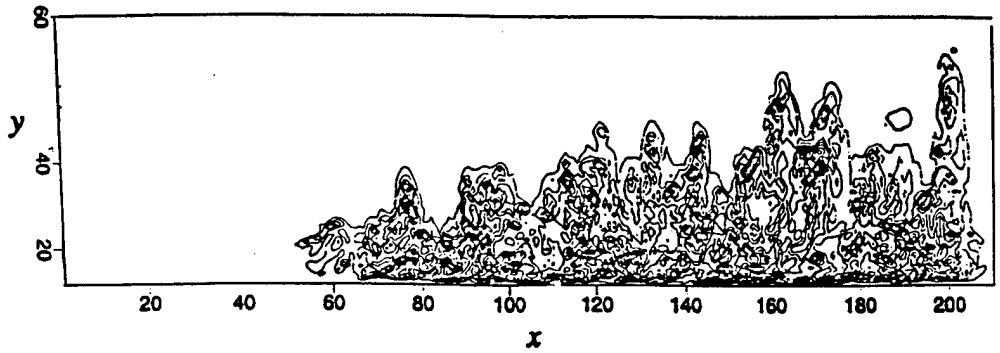

Figure 8. Plot of the eddy viscosity in the developing incompressible turbulent boundary layer obtained from LES (computations done by H. Fasel and co-workers at the University of Arizona).

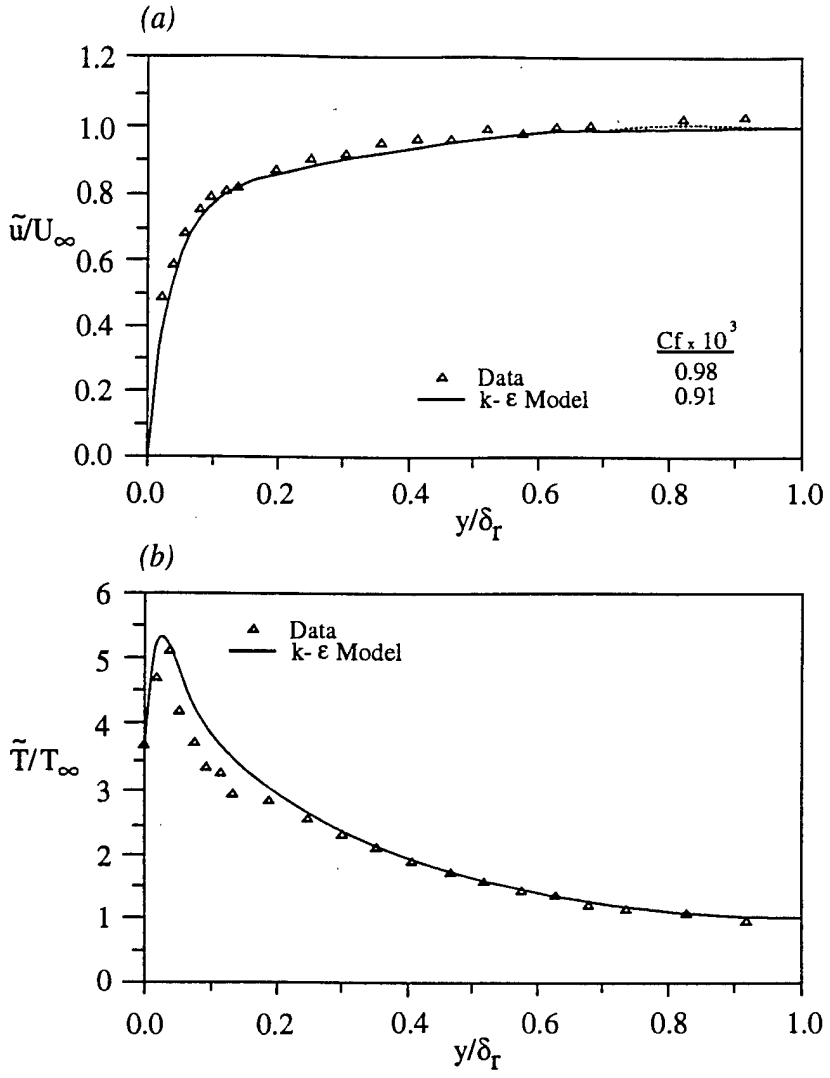

Figure 9. Comparison of the predictions of the new two-equation model as first computed by Zhang *et al.* (1993) for the compressible flat plate boundary layer with the experimental data of Kussoy and Horstman (1991) for $M_\infty = 8.18$ and $T_w/T_{aw} = 0.3$: (a) Mean velocity and (b) mean temperature.

REPORT DOCUMENTATION PAGE

Form Approved
OMB NO. 0704-0188

1. AGENCY USE ONLY *(Leave blank)*	2. REPORT DATE	3. REPORT TYPE AND DATES COVERED
	9/9/97	Technical Report 5/1/97 - 9/9/97

4. TITLE AND SUBTITLE

A COMBINED LARGE-EDDY SIMULATION AND TIME-DEPENDENT RANS CAPABILITY FOR HIGH-SPEED COMPRESSIBLE FLOWS

5. FUNDING NUMBERS

Contract No.

DAAG5597-1-0123

6. AUTHOR(S)

Charles G. Speziale

7. PERFORMING ORGANIZATION NAMES(S) AND ADDRESS(ES)

Department of Aerospace and Mechanical Engineering
Boston University
110 Cummington St.
Boston, MA 02215

8. PERFORMING ORGANIZATION REPORT NUMBER

AM-97-022

9. SPONSORING / MONITORING AGENCY NAME(S) AND ADDRESS(ES)

U.S. Army Research Office
P.O. Box 12211
Research Triangle Park,, NC 27709-2211

10. SPONSORING / MONITORING AGENCY REPORT NUMBER

11. SUPPLEMENTARY NOTES

The views, opinions and/or findings contained in this report are those of the author(s) and should not be construed as an official Department of the Army position, policy or decision, unless so designated by other documentation.

12a. DISTRIBUTION / AVAILABILITY STATEMENT

Approved for public release; distribution unlimited.

12 b. DISTRIBUTION CODE

13. ABSTRACT *(Maximum 200 words)*

An entirely new approach to the large-eddy simulation (LES) of high-speed compressible turbulent flows is presented. Subgrid scale stress models are proposed that are dimensionless functions of the computational mesh size times a Reynolds stress model. This allows a DNS to go continuously to an LES and then a Reynolds-averaged Navier-Stokes (RANS) computation as the mesh becomes successively more coarse or the Reynolds number becomes much larger. Here, the level of discretization is parameterized by the non-dimensional ratio of the computational mesh size to the Kolmogorov length scale. The Reynolds stress model is based on a state-of-the-art two-equation model whose enhanced performance is documented in detail in a variety of benchmark flows. It contains many of the most recent advances in compressible turbulence modeling. Applications to the high-speed aerodynamic flows of technological importance are briefly discussed.

14. SUBJECT TERMS	15. NUMBER IF PAGES
Turbulence; Large-Eddy Simulations	31
	16. PRICE CODE

17. SECURITY CLASSIFICATION OR REPORT	18. SECURITY CLASSIFICATION OF THIS PAGE	19. SECURITY CLASSIFICATION OF ABSTRACT	20. LIMITATION OF ABSTRACT
UNCLASSIFIED	UNCLASSIFIED	UNCLASSIFIED	UL